

## Article

# A Genome-Wide Analysis of Pathogenesis-Related Protein-1 (PR-1) Genes from *Piper nigrum* Reveals Its Critical Role during *Phytophthora capsici* Infection

Divya Kattupalli <sup>†</sup>, Asha Srinivasan <sup>†</sup> and Eppurath Vasudevan Soniya <sup>\*</sup>

Transdisciplinary Biology, Rajiv Gandhi Centre for Biotechnology, Thiruvananthapuram 695014, Kerala, India; divyak@rgcb.res.in (D.K.); ashas@rgcb.res.in (A.S.)

<sup>\*</sup> Correspondence: evsoniya@rgcb.res.in; Tel.: +91-471-252-9454; Fax: +91-471-234-8096<sup>†</sup> Contributed equally as the first Author.

**Citation:** Kattupalli, D.; Srinivasan, A.; Soniya, E.V. A Genome-Wide Analysis of Pathogenesis-Related Protein-1 (PR-1) Genes from *Piper nigrum* Reveals Its Critical Role during *Phytophthora capsici* Infection. *Genes* **2021**, *12*, 1007. <https://doi.org/10.3390/genes12071007>

Academic Editors: Chandrasekhar Natarajan, Neetha Nanoth Vellichirammal and Nishana Mayilaadumveettill

Received: 1 May 2021  
Accepted: 16 June 2021  
Published: 30 June 2021

**Publisher's Note:** MDPI stays neutral with regard to jurisdictional claims in published maps and institutional affiliations.



**Copyright:** © 2021 by the authors. Licensee MDPI, Basel, Switzerland. This article is an open access article distributed under the terms and conditions of the Creative Commons Attribution (CC BY) license (<https://creativecommons.org/licenses/by/4.0/>).

**Abstract:** Black pepper (*Piper nigrum* L.) is a prominent spice that is an indispensable ingredient in cuisine and traditional medicine. *Phytophthora capsici*, the causative agent of footrot disease, causes a drastic constraint in *P. nigrum* cultivation and productivity. To counterattack various biotic and abiotic stresses, plants employ a broad array of mechanisms that includes the accumulation of pathogenesis-related (PR) proteins. Through a genome-wide survey, eleven PR-1 genes that belong to a CAP superfamily protein with a caveolin-binding motif (CBM) and a CAP-derived peptide (CAPE) were identified from *P. nigrum*. Despite the critical functional domains, *PnPR-1* homologs differ in their signal peptide motifs and core amino acid composition in the functional protein domains. The conserved motifs of *PnPR-1* proteins were identified using MEME. Most of the *PnPR-1* proteins were basic in nature. Secondary and 3D structure analyses of the *PnPR-1* proteins were also predicted, which may be linked to a functional role in *P. nigrum*. The GO and KEGG functional annotations predicted their function in the defense responses of plant-pathogen interactions. Furthermore, a transcriptome-assisted FPKM analysis revealed *PnPR-1* genes mapped to the *P. nigrum*-*P. capsici* interaction pathway. An altered expression pattern was detected for *PnPR-1* transcripts among which a significant upregulation was noted for basic *PnPR-1* genes such as CL10113.C1 and Unigene17664. The drastic variation in the transcript levels of CL10113.C1 was further validated through qRT-PCR and it showed a significant upregulation in infected leaf samples compared with the control. A subsequent analysis revealed the structural details, phylogenetic relationships, conserved sequence motifs and critical cis-regulatory elements of *PnPR-1* genes. This is the first genome-wide study that identified the role of PR-1 genes during *P. nigrum*-*P. capsici* interactions. The detailed in silico experimental analysis revealed the vital role of *PnPR-1* genes in regulating the first layer of defense towards a *P. capsici* infection in Panniyur-1 plants.

**Keywords:** footrot; black pepper; promoter; cap domain; plant immunity; cis-regulatory element; biotic stress

## 1. Introduction

Plant immunity involves multiple layers of defense responses. The first layer of defense is triggered by the detection of microbe-associated molecular patterns (MAMPs) through plant-, pathogen- or pattern-recognition receptors (PRRs), which activate PAMP-/pathogen-/pattern-triggered immunity (PTI) [1]. The defense machinery of plants has been forced to evolve continuously to combat a wide range of abiotic and biotic stress factors. These challenges activate an array of induced mechanisms such as a hypersensitive response (HR), which involves a series of events including the production of reactive oxygen species (ROS) and the synthesis of antimicrobial molecules and pathogenesis-related (PR) proteins. PR proteins induce programmed cell death, which inhibits the spread of infection contributing to a systemic acquired resistance (SAR) [2,3]. In the second layer of

defense, pathogens suppress PTI by secreting the effector proteins that are later recognized by plant resistance (R) proteins leading to an effector-triggered immunity [1].

Salicylic acid and the subsequent activation of PR genes are necessary for the establishment of SAR in the distant regions of infections [4]. Arabidopsis mutants deficient in the non-expressor of pathogenesis-related 1 (*NPR1*) protein, a key SAR regulator, showed less PR gene expression, which, in turn, increased the susceptibility to pathogens. Various plant species overexpressing Arabidopsis *NPR1* displayed an enhanced disease resistance to pathogens such as *Rhizoctonia solani*, *Erwinia amylovora* and *Erysiphe necator* [5–7]. To date, 17 families of PR proteins have been classified and characterized [8]. PR proteins are functionally diverse proteins that are inducible during a pathogen attack and are regulated by signaling compounds such as abscisic acid (ABA), ethylene (ET), jasmonic acid (JA) and salicylic acid (SA) [9,10].

*PR-1a*, the first member of the *PR-1* family, was identified in *Nicotiana tabacum* plants infected with the tobacco mosaic virus. *PR-1* proteins belong to the group of the most abundantly produced proteins during plant defense responses and they are ubiquitous across plant species. *PR-1* proteins are involved in the cell wall thickening and thereby prevent the spread of the pathogens in the apoplast [11]. Apart from the biotic stresses, the role of *PR-1* in abiotic stresses [12] was also reported. During infections, the overexpression of *PR-1* proteins in the apoplast make them potential candidates for antimicrobial activity [13]. An enhanced tolerance to fungi [14], oomycetes [15] and bacterial infections [16] were demonstrated with an overexpression of *PR-1* in the transgenic plants. Apart from their role in various biotic and abiotic stresses *PR-1* and *PR-1*-like proteins have been reported to be involved in plant development, flowering and seed growth [17,18]. *PR-1* proteins are widely reported across the plant kingdom. These are the members of the cysteine-rich secretory protein, antigen 5, and the pathogenesis-related 1 (CAP) protein superfamily. Stress signaling peptides such as CAPE-1 (CAP-derived peptide 1) are embedded within *PR-1* proteins. A CAPE-1 peptide that comprised of the last 11 amino acids from the C-terminus of the *PR-1* protein was reported from tomato plants subjected to wounding and methyl jasmonate treatment [19]. A caveolin-binding motif (CBM) in the CAP region, which is involved in sterol binding, is responsible for antimicrobial activity against oomycetes including *Phytophthora* and *Pythium* species, which require exogenous sterols for basic metabolism. Plants with an enhanced *PR-1* expression are particularly well protected against oomycete pathogens [20]. The in-depth structural and biochemical analysis of *PR-1* proteins can provide greater insights into their function during defense signaling in crop plants.

In the world of spices, black pepper (*Piper nigrum* L., family Piperaceae) is considered to be the king of spices due to its pungent constituent. It is a major additive in many ayurvedic medicinal preparations besides its use as a preservative, a pesticide and a spice. The major hindrance in the *P. nigrum* production is the destructive footrot or quick wilt disease caused by an oomycete, *Phytophthora capsici* [21]. In this work, to extend our knowledge on the defense mechanisms underlying the PR function in *P. nigrum*, we carried out a comprehensive genome-wide analysis and validation of *PR-1* genes from *P. nigrum*. A transcriptome-assisted analysis and expression profiling revealed the differential expression of *PR-1* genes during *P. capsici* infection in *P. nigrum* variety Panniyur-1.

## 2. Materials and Methods

### 2.1. Identification and Analysis of *PR-1* Genes from the *P. nigrum* Genome

*PR-1* genes of *Arabidopsis thaliana* were downloaded from the TAIR (The Arabidopsis Information Resource) database (<https://www.arabidopsis.org/index.jsp>, accessed on 7 January 2021) and a tblastn search against the *P. nigrum* genome assemblies was performed [22]. The coding sequences were translated and aligned by a multiple sequence alignment using the BioEdit Sequence Alignment Editor [23]. The nucleotide and protein sequence conservations of all of the *PnPR-1* candidates were checked using Mega 7. The

domain structure prediction was carried out using an NCBI-Conserved Domain Database (CDD) [24].

The molecular weight and pI of *PnPR-1* proteins were estimated by the ExPASy ProtParam tool (<https://web.expasy.org/protparam/>, accessed on 15 January 2021). The potential signal peptide regions and the cleavage sites were also predicted using a SignalP 5.0 server (<http://www.cbs.dtu.dk/cgi-bin>, accessed on 15 January 2021). Subsequently, the conserved motifs of *PnPR-1* proteins were predicted using MEME (Multiple Em for Motif Elicitation) (<http://meme-suite.org/tools/meme>, accessed on 20 January 2021) [25].

## 2.2. GO and KEGG Analysis

Gene ontology (GO) was classified into biological processes, cellular components and the molecular function. The *PnPR-1* genes were analyzed for their role in GO using the PANNZER2 web server (<http://ekhidna2.biocenter.helsinki.fi/sanspanz/>, accessed on 25 January 2021) [26]. A KEGG (Kyoto Encyclopedia of Genes and Genomes) tool, BlastKOALA (KEGG Orthology and Links Annotation), a web server (<https://www.kegg.jp/blastkoala/>, accessed on 25 January 2021) [27], was used for the individual characterization of the gene functions.

## 2.3. Secondary and Tertiary Structure Prediction

The secondary structure prediction of the *PnPR-1* proteins was predicted using the Self-Optimized Prediction Method with Alignment (SOPMA) server ([https://npsa-prabi.ibcp.fr/cgi-bin/npsa\\_automat.pl?page=/NPSA/npsa\\_sopma.html](https://npsa-prabi.ibcp.fr/cgi-bin/npsa_automat.pl?page=/NPSA/npsa_sopma.html), accessed on 27 January 2021). The predicted 3D structures were built using a Protein Homology/analogy Recognition Engine v2 (Phyre2) server (<http://www.sbg.bio.ic.ac.uk/~phyre2/html/page.cgi?id=index>, accessed on 27 January 2021) [28]. The CASTp (Computed Atlas of Surface Topography of proteins) tool (<http://sts.bioe.uic.edu/castp/calculation.html>, accessed on 27 January 2021) was used to predict the active site pockets and topology of the *PnPR-1* protein structures [29].

## 2.4. Role of *PnPR-1* in *P. capsici*-Infected *P. nigrum*

The control *P. nigrum* (uninfected) leaf transcriptome data (SRA050094) and the *P. capsici*-infected *P. nigrum* leaf transcriptome data (SRX853366) were reanalyzed and the final assembled data were used for the expression studies. The *PnPR-1* sequences curated from the *P. nigrum* genome [22] were mapped to the transcriptome assembly files. The differential regulation of the obtained transcripts was checked using FPKM (fragments per kilobase of transcript per million mapped reads) values.

## 2.5. Plant-Pathogen Infections, Staining and RT-qPCR

Virulent, pure cultures of *P. capsici* and root cuttings of the *P. nigrum* cultivar Panniyur-1 were obtained from the College of Agriculture, Vellayani. *P. capsici* was subcultured every 15 days on potato dextrose agar (PDA) and stored at 28 °C. A 48 h old *P. capsici* culture in PDA was used in this study. *P. capsici* mycelial discs were used to infect the fully-expanded second leaf of the *P. nigrum* plant. The mock treatments were replaced with plain PDA discs. Mock-infected plants were used as a control. The infected leaf samples were collected at 6 h, 12 h and 24 h after infection. The mock samples were collected at 24 h. To detect and visualize the tissue damage in the leaf region after 24 h of pathogen infection, trypan blue staining was performed [30]. Three biological replicates were used for all of the studies.

At each timepoint, the leaf samples were collected and flash frozen in liquid nitrogen and stored at −80 °C until use. Total RNA was isolated from the collected leaf samples using a mirVana miRNA isolation kit (Invitrogen, Cat No: AM1560) according to the manufacturer's instructions. The quality and the concentration of the RNA samples were checked by using a Colibri Microvolume Spectrometer. The RNA was reverse-transcribed into cDNA using a high-capacity cDNA synthesis kit (Applied Biosystems, Cat No: 4374966). RT-qPCR was carried out using the Applied Biosystems 7900 HT sequence

detection system (ABI) using SYBR Green qPCR Master Mix (ABI). Each qPCR reaction was conducted in a 10  $\mu$ L volume containing 1  $\mu$ L of diluted cDNA (10 ng/ $\mu$ L), 5  $\mu$ L of SYBR green and 5 pmol of forward (TCTTGTTGTTCCGAGCCCTAG) and reverse primer (GCGTAATCCCGTCCGTAGGT) with the following conditions: 40 cycles of 95 °C for 15 s DNA denaturation, annealing at 60 °C for 15 s and elongation at 72 °C for 30 s. The 5.8S RNA was used as an endogenous control [31]. The relative quantification was analyzed by the comparative CT method using the formula  $2^{-\Delta\Delta CT}$  and the standard deviation was represented as the error bar [32].

### 2.6. Prediction of cis-Acting Regulatory Elements in Promoter Regions

The genomic sequences of the 2.0 kbp upstream of the coding sequence (CDS) region of each *PnPR-1* gene were extracted from the *P. nigrum* genome assembly. The promoter regions of each *PR1* gene were scanned for the presence of functional motifs using Softberry ([http://www.softberry.com/berry.phtml?topic=case\\_study\\_plants&no\\_menu=on](http://www.softberry.com/berry.phtml?topic=case_study_plants&no_menu=on), accessed on 30 January 2021) and New PLACE (<https://www.dna.affrc.go.jp/PLACE/?action=newplace>, accessed on 30 January 2021) [33].

## 3. Results

### 3.1. Genome-Wide Identification and Analysis of *P. nigrum* *PR-1* Genes

Eleven potential *PnPR-1* gene candidates were obtained from the genome-wide analysis in comparison with the *A. thaliana* *PR* genes. The number of exons in each *PnPR-1* gene is one except in Pn2.357, which has two exons. The basic information of the *PnPR-1* genes including the protein sequence length, isoelectric points and molecular weight are listed in Table 1. The length of the *PnPR-1* proteins ranged from 127 to 357 amino acid residues with a molecular weight ranging from 14.38 to 38.49 kDa. The theoretical isoelectric point (pI) data categorized the majority of the *PnPR-1* proteins into basic except Pn21.1032 and Pn36.35 that were acidic. The extreme acidic or basic properties can contribute to distinct functions of each *PnPR-1* gene. Five gene loci for *PnPR-1* were distributed in the *P. nigrum* genome scaffold 23. Furthermore, the signal peptide regions and cleavage sites were also identified in all of the *PnPR-1* protein sequences except Pn11.1637 and Pn31.171 (Table 2). All of the *PnPR-1* genes that were mapped to scaffold 23 had the same signal peptide cleavage positions in between the 24th and 25th amino acids.

**Table 1.** Sequence characteristics and physio-chemical properties of the *PR-1* proteins in *Piper nigrum*.

| Genome CDS Id | Genome Scaffold No. | Exon No. | Start    | Stop     | Strand | Protein Length (AA) | Molecular Weight (kDa) | Theoretical pI |        |
|---------------|---------------------|----------|----------|----------|--------|---------------------|------------------------|----------------|--------|
| Pn2.460       | Pn23                | 1        | 1315655  | 1316146  | –      | 155                 | 17.09488               | 4.82           | Acidic |
| Pn2.459       | Pn23                | 1        | 1320928  | 1321419  | –      | 192                 | 21.91361               | 5.8            |        |
| Pn2.433       | Pn23                | 1        | 1493563  | 1494054  | –      | 168                 | 18.35074               | 7.58           |        |
| Pn2.357       | Pn23                | 2        | 2226595  | 2229193  | –      | 127                 | 14.37881               | 7.62           |        |
| Pn2.340       | Pn23                | 1        | 2402850  | 2403341  | –      | 185                 | 19.80756               | 9.1            |        |
| Pn21.1032     | Pn3                 | 1        | 3202437  | 3202904  | +      | 163                 | 17.85002               | 9.15           | Basic  |
| Pn31.171      | Pn15                | 1        | 26854949 | 26855332 | –      | 163                 | 17.87807               | 9.3            |        |
| Pn36.35       | Pn25                | 1        | 5754975  | 5755553  | –      | 163                 | 17.88005               | 9.3            |        |
| Pn11.1637     | Pn4                 | 1        | 33322945 | 33323502 | –      | 176                 | 19.63337               | 9.37           |        |
| Pn8.549       | Pn8                 | 1        | 25779763 | 25780269 | –      | 163                 | 17.96421               | 9.44           |        |
| Pn14.1312     | Pn14                | 1        | 5932334  | 5932864  | +      | 357                 | 38.49596               | 11.3           |        |

**Table 2.** Signal peptide region detected from the *PnPR-1* proteins.

| Genome Id | Cleavage Site Position | Sequence Position | Probability | Protein Type | Signal Peptide (Sec/SPI) | Other  |
|-----------|------------------------|-------------------|-------------|--------------|--------------------------|--------|
| Pn21.1032 | 16 and 17              | CNA-QN            | 0.9541      | Likelihood   | 0.9981                   | 0.0019 |
| Pn2.340   | 24 and 25              | AQA-QN            | 0.8849      | Likelihood   | 0.9984                   | 0.0016 |
| Pn2.357   | 24 and 25              | AQA-QN            | 0.8898      | Likelihood   | 0.9986                   | 0.0014 |
| Pn2.433   | 24 and 25              | AQA-QN            | 0.8892      | Likelihood   | 0.9987                   | 0.0013 |
| Pn2.459   | 24 and 25              | AQA-QN            | 0.8898      | Likelihood   | 0.9986                   | 0.0014 |
| Pn2.460   | 24 and 25              | AQA-QN            | 0.8892      | Likelihood   | 0.9987                   | 0.0013 |
| Pn36.35   | 29 and 30              | ASS-SP            | 0.6292      | Likelihood   | 0.9813                   | 0.0187 |
| Pn14.1312 | 31 and 32              | TNA-AL            | 0.4399      | Likelihood   | 0.7324                   | 0.2676 |
| Pn8.549   | 30 and 31              | TLA-QN            | 0.3454      | Likelihood   | 0.5106                   | 0.4894 |
| Pn31.171  | -                      | -                 | -           | Likelihood   | 0.0029                   | 0.9971 |
| Pn11.1637 | -                      | -                 | -           | Likelihood   | 0.2691                   | 0.7309 |

The multiple sequence alignment of all of the eleven *PnPR-1* proteins revealed highly conserved CAP domain sequences, which further confirmed that these candidates belonged to the CAP superfamily. The CAP domain structure comprises of about 150 amino acids and also include a caveolin-binding motif (CBM) and a CAP-derived peptide (CAPE) motif (Figure 1). A comparison of the *PnPR-1* sequences with various other monocot and dicot plants showed a distinct CAP domain with a CBM and a CAPE (Supplementary Figure S1) in *P. nigrum*. A SignalP analysis revealed about 24 amino acid long signal peptide regions (pink colored boxes) of *PnPR-1* at the N terminal side. The predicted cleavage site is indicated by the arrowhead.



**Figure 1.** Multiple sequence alignments of the *PnPR-1* protein sequences. The pink colored rectangle boxes indicate the signal peptide regions; the cleavage sites predicted are indicated by the blue arrowheads. The green line indicates the CAP domain structure of ~150 bp. The yellow and blue color rectangles show the caveolin-binding motif (CBM) and CAP-derived peptide (CAPE), respectively.

### 3.2. Sequence Conservation of *PnPR-1* Genes

The subsequent phylogenetic analysis of all eleven *PR-1* nucleotide and protein sequences through the maximum-likelihood method with 1000 bootstraps (Supplementary Figure S2A,B) revealed two main clusters leaving one outnumbered group (Pn21.1032). A total of ten conserved motifs were identified using the MEME server. Motifs 1 and 2 were conserved in all of the deduced *PR-1* proteins whereas motif 3 and motif 6 were conserved in all *PnPR-1* proteins except in Pn31.171 and Pn2.357, respectively. Motif 8, motif 9 and motif 10 were preserved in Pn36.35 along with Pn14.1312, Pn31.171 and Pn11.637, respectively (Figure 2).

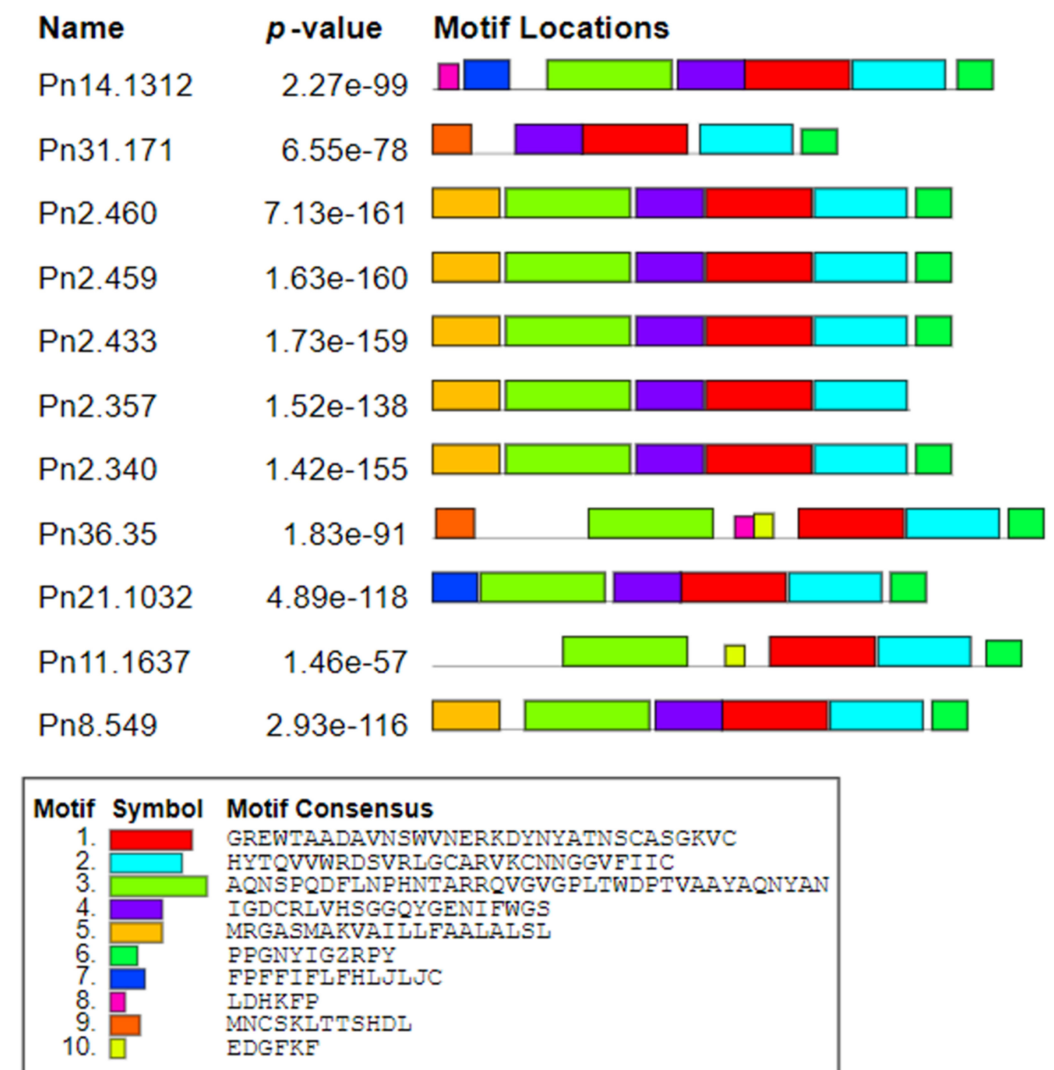


**Figure 2.** Conserved motifs identified from *Piper nigrum PR-1* protein homologs.

A total of 10 conserved motifs were identified. Each color represents different motifs with consensus sequences.

### 3.3. GO and KEGG Pathway Analysis of *PnPR-1* Genes

A gene ontology (GO) analysis yielded five biological processes, four molecular functions and four cellular components. Based on the GO enrichment analysis, most of the *PR-1* genes had their role in defense responses and a response to a biotic stimulus in a biological function. In terms of the molecular function, it had protein kinase activity and adenylyl nucleotide and purine ribonucleoside-binding activities. The cellular component showed its role in the extracellular region (Table 3). A KEGG pathways analysis categorized

its role in the environmental information processing signal transduction pathways such as the MAPK signaling pathway (plant 04016), the plant hormone signal transduction (04075) and the plant-pathogen interaction (04626).

**Table 3.** The gene ontology (GO) term distribution of *PnPR-1* proteins.

| GO ID      | GO Domain          | Function Description                       |
|------------|--------------------|--|
| GO:0006952 | Biological process | Defense response                           |
| GO:0009607 | Biological process | Response to biotic stimulus                |
| GO:0048544 | Biological process | Recognition of pollen                      |
| GO:0006468 | Biological process | Protein phosphorylation                    |
| GO:0010274 | Biological process | Hydrotropism                               |
| GO:0004672 | Molecular function | Protein kinase activity                    |
| GO:0030554 | Molecular function | Adenyl nucleotide binding                  |
| GO:0035639 | Molecular function | Purine ribonucleoside triphosphate binding |
| GO:0032555 | Molecular function | Purine ribonucleotide binding              |
| GO:0005576 | Cellular component | Extracellular region                       |
| GO:0016020 | Cellular component | Membrane                                   |
| GO:0031224 | Cellular component | Intrinsic component of membrane            |

### 3.4. Secondary and 3D Structure of the *PnPR-1* Protein

A varied percentage of  $\alpha$ -helices (15.6–36.88%), extended strands (10.64–23.78%),  $\beta$ -turns (3.65–5.88%) and random coils (37.42–67.79%) were found in the *Pn-PR1* proteins (Supplementary Figure S3). The relative proportion of the structural features differed among the *PnPR-1* proteins. Pn31.171 and Pn2.357 showed less  $\alpha$ -helix structures and more random coils compared with the other counterparts. Despite the 3D structural variations detected among the *PnPR-1* proteins (Figure 3), the binding pockets critical for protein interaction were found in all of the eleven candidates. At the same time, the proportion of disordered regions of *PR-1* proteins ranged from 4.5–28.1%.

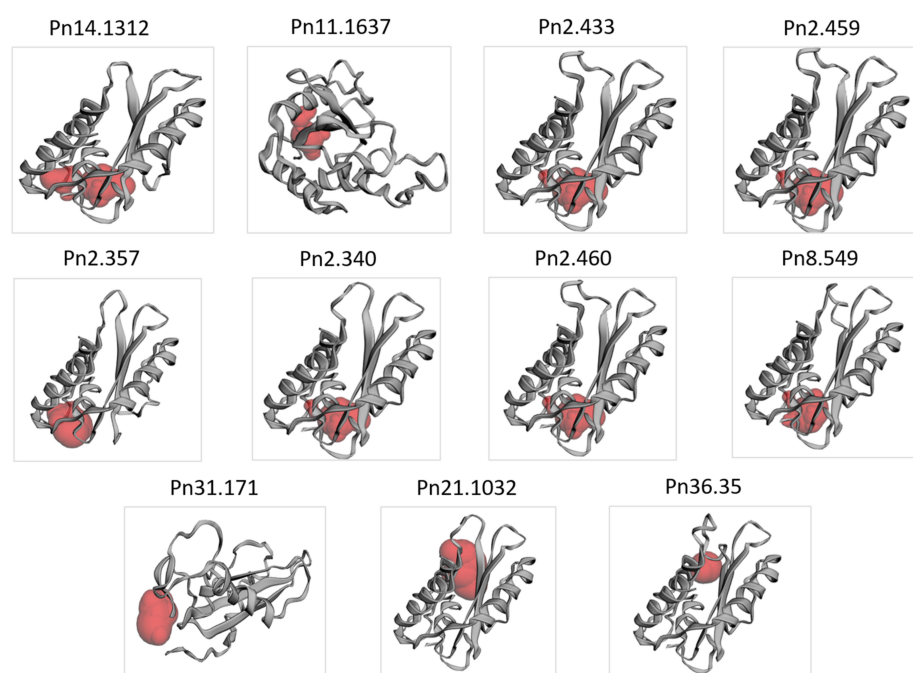


**Figure 3.** The predicted 3D structures of *PnPR-1* proteins generated using the Phyre2 server and binding pockets identified by the CASTp 3.0 server (red color).

### 3.5. Cis-Regulatory Elements of the *PnPR-1* Genes

The cis-elements were found to be distributed over the 2.0 kb upstream promoter region of the *PnPR-1* genes (Figure 4) except in Pn2.357. The length of these cis-elements varied from 9 to 42 bp in the Softberry database whereas they were 4 to 24 bp in the New PLACE database. This was compared with the length of the cis-elements in *A. thaliana* (4–13 bp) and in *O. sativa* (4–10 bp) carried out by using the PlantCare program [34]. Among the ten *PR-1* gene loci, the typical TGA binding site LS7, WBSI, G-box and C-motif were found in the promoter regions of Pn36.35. Meanwhile, the GT motif and Zc2A/T-2 were found in Pn2.340, Pn2.433 and Pn2.460. The hormone signaling elements such as ABI4 and GCC-box were present in Pn2.459, Pn2.340 and Pn2.433, respectively. The stress-responsive MYB was also detected in the promoter regions of the *PnPR-1* genes such as Pn21.1032, Pn31.171 and Pn36.35. Among the 154 cis-elements detected from the New PLACE database, the CAAT box (CAAT), E-box (CANNTG) and DOFCOREZM (AAAG) regions were found to be widely distributed across the *PnPR-1* promoter regions (Supplementary Figure S4).

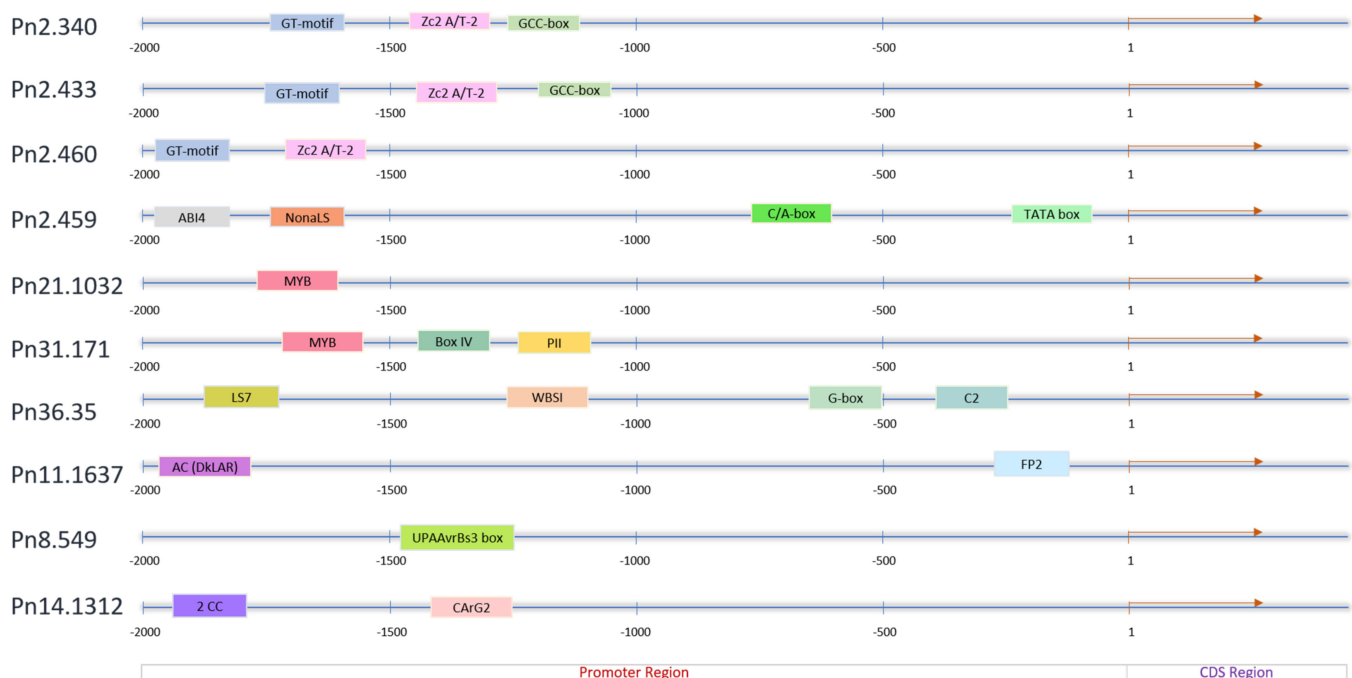


**Figure 4.** Analysis of the cis-acting elements of the *PnRR-1* promoter regions (2 kb upstream from the CDS region) using Softberry software. Each element is represented with different colors.

### 3.6. Expression of *PR-1* Genes during *P. capsici* Infection in *P. nigrum*

The assembled transcriptome of the RNA-seq data from the control (NCBI-SRA050094) and the *P. capsici*-infected *P. nigrum* (NCBI-SRX853366) plants revealed 60,437 transcripts. From the assembled data, seven transcripts of the *PnPR-1* genes were mapped to the *P. capsici*-*P. nigrum* interaction pathway. The transcript lengths ranged from 391–1015 bps. A differential expression of these transcripts between the control leaf (CL) and the infected leaf (IL) was assessed from their corresponding FPKM values. CL10113.C1/2 and Unigene17664 were mapped to the Pn23 and Pn8 scaffolds, respectively, and were significantly upregulated ( $p$ -value < 0.01) in the IL compared with the CL. Meanwhile, Unigene11116, Unigene15555, Unigene26912 and Unigene693 were significantly downregulated ( $p$ -value < 0.01) in the IL compared with the CL (Figure 5).

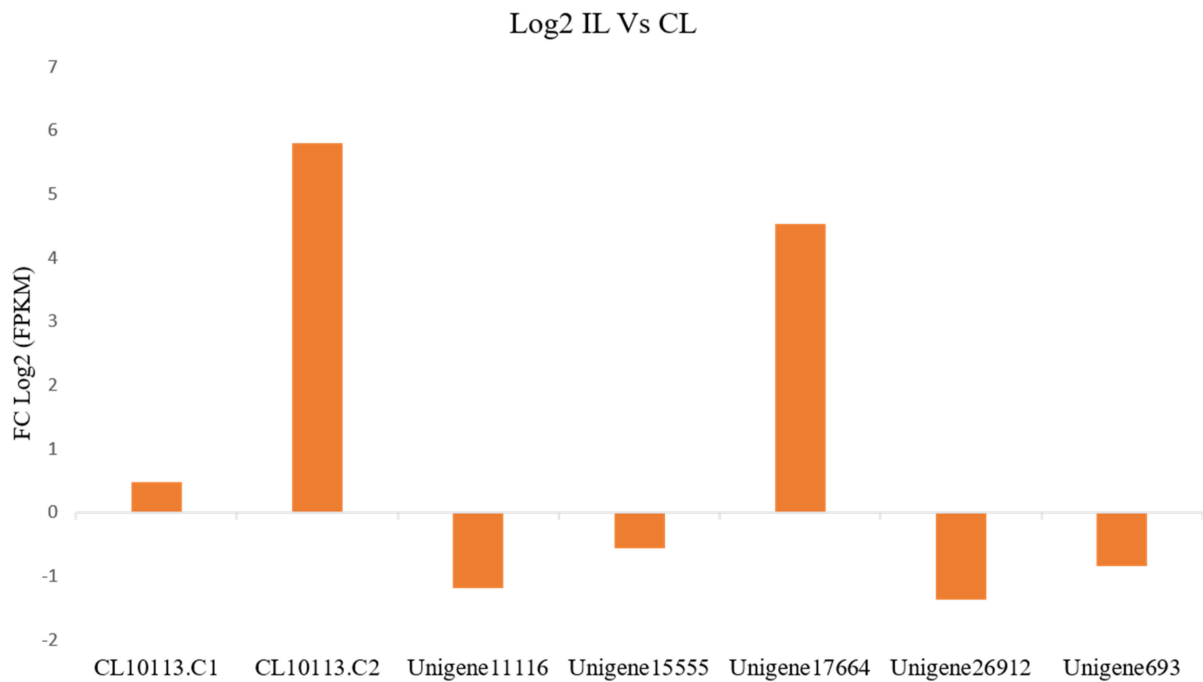


**Figure 5.** Expression analysis of the *PnPR-1* transcripts in *Phytophthora capsici*-infected *P. nigrum* using FPKM (fragments per kilobase of transcript per million mapped reads) values. From the left, the *PnPR-1* transcripts are designated as CL10113.C1, CL10113.C2, Unigene11116, Unigene15555, Unigene17664, Unigene26912 and Unigene693. Positive and negative numbers on the X-axis indicate the fold changes in the Log<sub>2</sub> gene expression levels.

### 3.7. Trypan Blue Staining and Microscopic Detection of *P. capsici* Infection

The development of necrotic lesions was detected on *P. nigrum* leaves after the *P. capsici* infection. As the lesion size progressed with the infection, the pathogen spores were profusely developed from the infected tissues. *P. capsici*-induced cell death on *P. nigrum* leaves was detected using trypan blue staining. The infected tissue was stained in blue whereas the viable cells were colorless (Figure 6B).

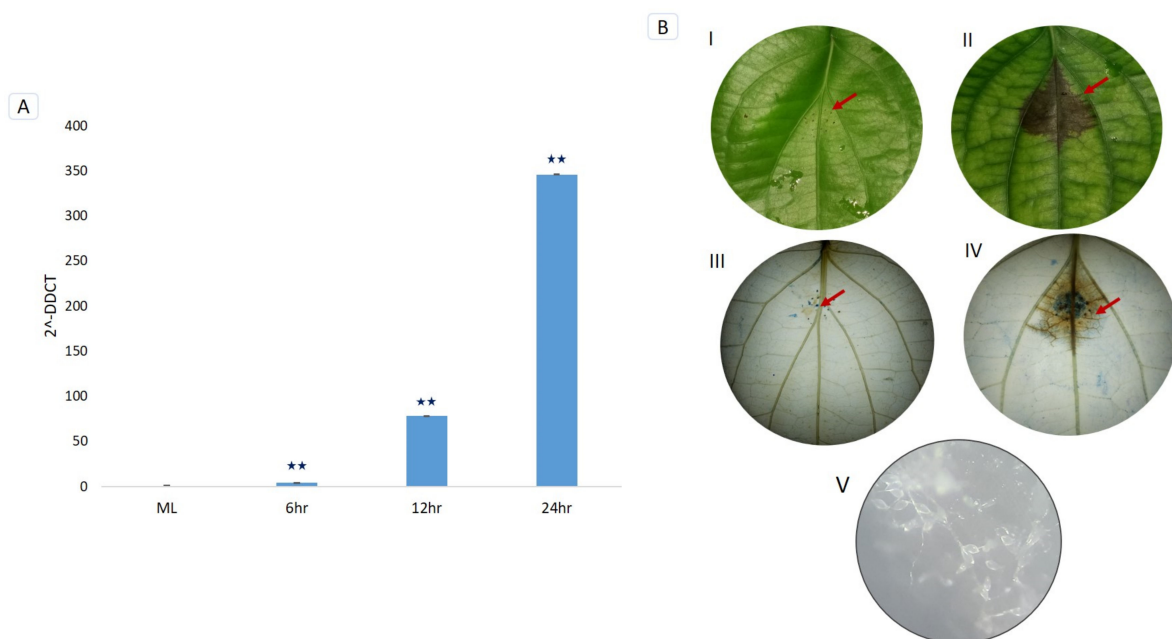


**Figure 6.** (A) Temporal expression validation of CL10113.C2 *PnPR-1* gene in *Phytophthora capsici*-infected *Piper nigrum* plants by RT-qPCR. ML (mock-infected leaf) 6 hpi (hours post-infection), 12 hpi and 24 hpi. Asterisks indicate significant changes

( $p$ -value < 0.001). (B) Mock and *Phytophthora capsici*-infected *Piper nigrum* leaves after 24 h of infection. (I) Mock-infected leaf. (II) *Phytophthora capsici*-infected *Piper nigrum* leaf. (III) Trypan blue-stained mock-infected leaf. (IV) Trypan blue-stained infected leaf. (V) *Phytophthora capsici* spores developed from the infected tissues. Red colored arrows indicate the infected regions.

### 3.8. RT-qPCR Validation of PnPR-1 Genes

We validated the relative expression of the remarkably upregulated *PnPR-1* gene (CL10113.C2; Figure 5) using RT-qPCR from *P. capsici*-infected *P. nigrum* and mock control (ML) plants. The temporal expression at 6 h, 12 h and 24 h of *P. capsici* infections revealed a differential expression of the *PnPR-1* (CL10113.C2) gene. A significant (>0.001) upregulation of the *PnPR-1* gene (CL10113.C2) was observed in the leaves at 6 hpi, 12 hpi and 24 hpi compared with the mock control plants (Figure 6A).

## 4. Discussion

PR proteins are defense-related signaling molecules induced by phytopathogens that play a vital role in resisting the entry of the invading pathogen. PR proteins have been classified into many families based on their function, molecular weight, amino acid sequence and other properties [35]. In tobacco, PR proteins were initially classified as five major classes (PR1, PR2, PR3, PR4 and PR5) [36]. However, later studies in tobacco and the tomato have grouped them into 11 families [37]. The members belonging to the PR family can be either acidic or basic. Basic PR proteins are located intracellularly in the vacuole regions and are constitutively expressed to some extent and are also induced by stress signals whereas acidic types are produced extracellularly and only triggered by specific stress signals [38]. In our current study, both acidic and basic *PR-1* proteins, which have a critical role during *P. nigrum*-*Phytophthora* interactions, were identified. The majority detected were basic in nature; this was the same as in the case of the *PR1* proteins studied in *S. lycopersicum* during drought stress [12]. Contrasting to this, a greater number of acidic *PR1* genes were also reported from rice, where among 12 *PR1* rice protein candidates seven were acidic in nature [39]. In *Glycine max* during multiple biotic and abiotic stresses among 24 *PR1* proteins, 15 were detected as acidic [40].

A KEGG orthology analysis revealed *P. nigrum PR-1* genes mapped to the plant-pathogen interaction (04626), MAPK signaling pathway (04016) and plant hormone signal transduction (04075). The *PR-1* family mainly possesses antifungal and anti-oomycete activities [35]. The overexpression of *PR1* or similar proteins in various plants leads to an enhanced disease resistance to a wide variety of pathogens [39], especially the oomycetes [15]. The anti-oomycete properties of *PR-1* proteins such as P14c and *PR-1* were demonstrated against the sterol auxotroph pathogen *Phytophthora brassicae* [20].

As previously reported [13,20], *P. nigrum PR-1* proteins possess the CAP tetrad, the CBM involved in sterol binding [41] and the CAPE involved in plant immune signaling [19]. The ability of the *PR-1* family of proteins to bind sterols contributes towards their antimicrobial activity towards the *Phytophthora* species, a major plant pathogen belonging to the sterol auxotroph [20]. The CAPE-1 peptide has the consensus motif PxGNxxxxPY, which is conserved between the monocots and dicots. A highly conserved and distinct similarity in the domains of the protein structure was observed in *PnPR-1* proteins, which might account for a general strategy in responding to various biotic stresses as reported in other studies [42]. The role of the CAPE-1 peptide in the defense signaling was demonstrated in a previous study on the *Pseudomonas syringae* pv tomato (Pst) strain DC3000 interaction in tomatoes. A diverse set of defense-related genes was induced in the tomato plants pretreated with the CAPE-1 peptide. Furthermore, a non-canonical pathway other than PAMP-triggered immunity (PTI) signaling was suggested for the CAPE-1 mediated defense responses as the CAPE-1 did not induce the WRKY transcription factor 53 (WRKY53) [19]. The pathogen effector ToxA and Tox3 proteins from *Parastagonospora nodorum* were found to interact with wheat *PR-1* proteins [43,44]. Promoters are the regulators of a gene at the transcriptional level [45]. Various computational methods are thoroughly being used for

the identification of different cis-elements in the promoter region that are responsible for the regulation of genes [46]. A range of cis-elements was predicted from *P. nigrum* *PR-1* genes, which were likely related to the regulation of the plant growth, development and response to various stresses. A high frequency of the CAAT box (CAAT), E-box (CANNTG) and DOFCOREZM (AAAG) regions was found in the *PnPR-1* promoter regions. A high occurrence of the CAAT box was previously reported in *A. thaliana* PR proteins [34]. As previously reported, hormone-regulating sequence motifs [45] such as LS7, GCC-box, ABA-responsive elements (ABREs; also termed as G-box) [47] and ABI4 were detected from the upstream of certain *PnPR-1* genes. LS7, which contains a TGA binding site, has been reported to be the key activator of *PR-1* expression, NPR1 [48]. The ethylene-responsive factor binds to the GCC-box (ethylene-responsive element) and responds to various biotic and abiotic factors in Arabidopsis [49]. The ABA-insensitive-4 (ABI4) transcription factor was reported to be involved in ascorbate-dependent plant growth [50]. AC elements in the promoter region of the Leucoanthocyanidin reductase gene in the Proanthocyanidin pathway promoter harbors the binding site for MYB2 Myb-like transcription factors [51]. Subsequently, the WER-binding site (WBSI) and NonaLS are also reported in the *PnPR-1* promoter region. WBSI was detected in the *CAPRICE* (*CPC*) promoter of Arabidopsis. WEREWOLF (WER) is a MYB protein and gene transcription activator during the specification of epidermal cell fates [52]. NonaLS (Nona-like sequence, GATCGGACG) is the positive cis-acting element of histone *H1* genes in wheat, tomato and Arabidopsis [53]. The induction of both biotic- and abiotic-responsive cis-acting regulatory elements in *PnPR-1* indicates that these genes play a key role in regulating resistance against *P. capsici* and other abiotic stresses in *P. nigrum*.

Even though *PR-1* proteins belong to the group of abundant proteins expressed in the plant-pathogen interaction, all of the members of the family were not uniformly upregulated [13]. Likewise, a transcriptome-assisted analysis revealed a high upregulation of two basic *PR-1* genes ( $pI > 7.35$ ) such as CL10113.C1/2 and Unigene17664 in *P. nigrum* upon *P. capsici* infection. As *PR-1* genes belong to the group of multigene families, they differ widely in their properties. *PR-1* expression levels rise both transcriptionally and translationally upon pathogen infections [54,55]. Consistent with previous studies, the upregulation of *PnPR-1* transcripts such as CL10113.C1, CL10113.C2 and Unigene17664 were detected during *P. capsici* infection in *P. nigrum*. The qRT-PCR expression studies also validated the drastically increased CL10113.C2 expression pattern at 24 hpi (Figure 6A). The significant upregulation of *PR1* in *P. nigrum*-infected *P. capsici* showed similar expression patterns in the case of *Brassica juncea* and *Erysiphe cruciferarum* pathogen interaction where the expression of *PR1* was strongly upregulated [56]. This resembles the mechanism of PR genes being upregulated following pathogen infection, indicating that *P. capsici* actively works in manipulating the *P. nigrum* host defenses. In addition to the host defense response during pathogen infection, *PR-1* proteins were also reported to have a role in abiotic stress stimuli [57–59].

The trypan blue staining clearly showed the necrotic region as the defense response of the host plant to the pathogen and its further effect to inhibit the growth of the pathogen to the surrounding regions (Figure 6B). This was, in turn, proved by the significant upregulation of the *PnPR-1* genes at 24 h post-infection in the leaf samples using qPCR experiments. To date, only a few studies have been carried out on the role of PR proteins in *P. nigrum* or related Piperaceae species. The activity of PR protein chitinase,  $\beta$ -1,3-glucanase and their related enzymes were reported in *P. capsici*-infected *P. nigrum* plants [60–62]. The present study contributes a significant advancement in the understanding of the molecular function of *PR-1* proteins in *P. nigrum*. *PnPR-1* genes are found to have a key role in the early defense such as PTI towards *P. capsici* infection in Panniyur-1 plants. It may be possible that the key genes in the subsequent effector-triggered immunity act as critical players of the defense response in Panniyur-1 plants. Therefore, future studies on the identification of the potential *P. capsici* effectors coupled with *PR-1* functional studies will

ascertain the in-depth mechanisms of the defense signal amplification and anti-oomycete properties of these enigmatic proteins in *P. nigrum*.

## 5. Conclusions

The genome-wide survey identified eleven *P. nigrum* *PR-1* gene homologs mapped to seven distinct genome scaffolds. A subsequent transcriptome analysis of *P. capsici*-infected *P. nigrum* plants showed the expression of *PR-1* genes from all of the mapped loci. Our study revealed the differential regulation of *PR-1* gene candidates in *P. capsici*-infected *P. nigrum* plants. A significant upregulation was detected for the transcripts of certain *PnPR-1* genes such as CL10113.C2 and Unigene17664. A detailed in silico analysis revealed cis-regulatory elements such as phytohormone-responsive transcription activators in the promoter regions. The structural analysis revealed similar binding pockets in the predicted 3D structures of all *PnPR-1* proteins except Pn31.171. The differential expression of certain *PnPR-1* homologs revealed their crucial role during the early defense response in the *P. capsici*-*P. nigrum* interaction. Further in-depth functional studies on *PnPR-1* genes, promoter cis-regulatory elements and the pathogen-specific effectors can provide the exact molecular mechanism of the susceptibility/tolerance of *P. nigrum* cultivars to Phytophthora infection, which, in turn, can contribute towards the novel disease protection strategies in *P. nigrum* plants.

**Supplementary Materials:** The following are available online at <https://www.mdpi.com/article/10.3390/genes12071007/s1>, Figure S1: The amino acid sequences from *Piper nigrum*, *Nymphaea colorata*, *Elaeis guineensis*, *Cinnamomum micranthum*, *Gossypium tomentosum*, *Musa ABB*, *Amborella trichopoda* and *Phoenix dactylifera* were aligned using Geneious bioinformatics software (<https://www.geneious.com/>, accessed on 28 January 2021) with default settings. The conserved domains are highlighted in different colors. The CAP domain structure with a caveolin-binding motif (CBM) and a CAP-derived peptide (CAPE) are shown in red and pink boxes; Figure S2: Phylogenetic analyses of *Piper nigrum* *PR-1* nucleotide and protein sequences. The phylogenetic tree was constructed using MEGA 7.0. by the maximum-likelihood (ML) method with 1000 bootstrap replicates and default parameters. The *PnPR-1* family genes were divided into two major groups, groups I and II; Figure S3: Secondary structure analyses of *PnPR-1* proteins; Figure S4: Analysis of cis-acting elements in *PnPR-1* promoters using the New PLACE online server. The number of elements in each gene is represented in data bars.

**Author Contributions:** D.K., A.S. and E.V.S. conceived the research plans and designed the experiments. D.K. and A.S. performed the experiments, analyzed the data and wrote the article, E.V.S. made critical revisions. All authors have read and agreed to the published version of the manuscript.

**Funding:** This work was supported by the Department of Biotechnology (DBT), India. The funders have no role in study design, data collection and analysis, decision to publish or preparation of the manuscript.

**Institutional Review Board Statement:** Not applicable.

**Informed Consent Statement:** Not applicable.

**Data Availability Statement:** Control *P. nigrum* (uninfected) leaf transcriptome data and *P. capsici*-infected *P. nigrum* leaf transcriptome data can be accessed from NCBI SRA, accession numbers SRA050094 and SRX853366, respectively.

**Acknowledgments:** K.D. acknowledges the Department of Biotechnology (DBT)—JRF and SRF and Commonwealth Scholarship Commission (CSC) for a split-site scholarship. S.A. greatly acknowledges the fellowship from the Council of Scientific and Industrial Research (CSIR)—JRF and SRF (S.A.). E.V.S. acknowledges financial support from DBT, New Delhi.

**Conflicts of Interest:** The authors declare no conflict of interest.

## References

1. Dangl, J.L.; Jones, J.D.G. Plant pathogens and integrated defence responses to infection. *Nature* **2001**, *411*, 826–833. [[CrossRef](#)] [[PubMed](#)]
2. Van Baarlen, P.; Van Belkum, A.; Summerbell, R.C.; Crous, P.W.; Thomma, B.P. Molecular mechanisms of pathogenicity: How do pathogenic microorganisms develop cross-kingdom host jumps? *FEMS Microbiol. Rev.* **2007**, *31*, 239–277. [[CrossRef](#)]
3. Chassot, C.; Nawrath, C.; Métraux, J.-P. Cuticular defects lead to full immunity to a major plant pathogen. *Plant J.* **2007**, *49*, 972–980. [[CrossRef](#)] [[PubMed](#)]
4. Boccoardo, N.A.; Segretin, M.E.; Hernandez, I.; Mirkin, F.G.; Chacón, O.; Lopez, Y.; Borrás-Hidalgo, O.; Bravo-Almonacid, F.F. Expression of pathogenesis-related proteins in transplastomic tobacco plants confers resistance to filamentous pathogens under field trials. *Sci. Rep.* **2019**, *9*, 1–13. [[CrossRef](#)] [[PubMed](#)]
5. Le Henanff, G.; Farine, S.; Kieffer-Mazet, F.; Miclot, A.-S.; Heitz, T.; Mestre, P.; Bertsch, C.; Chong, J. *Vitis vinifera* VvNPR1.1 is the functional ortholog of AtNPR1 and its overexpression in grapevine triggers constitutive activation of PR genes and enhanced resistance to powdery mildew. *Planta* **2011**, *234*, 405–417. [[CrossRef](#)]
6. Molla, K.A.; Karmakar, S.; Chanda, P.; Sarkar, S.N.; Datta, S.K.; Datta, K. Tissue-specific expression of Arabidopsis NPR1 gene in rice for sheath blight resistance without compromising phenotypic cost. *Plant Sci.* **2016**, *250*, 105–114. [[CrossRef](#)] [[PubMed](#)]
7. Malnoy, M.; Jin, Q.; Borejsza-Wysocka, E.E.; He, S.Y.; Aldwinckle, H.S. Overexpression of the apple MpNPR1 gene confers increased disease resistance in *Malus x domestica*. *Mol. Plant Microbe Interact.* **2007**, *20*, 1568–1580. [[CrossRef](#)] [[PubMed](#)]
8. Christensen, A.B.; Cho, B.H.O.; Næsby, M.; Gregersen, P.L.; Brandt, J.; Madriz-Ordeñana, K.; Collinge, D.B.; Thordal-Christensen, H. The molecular characterization of two barley proteins establishes the novel PR-17 family of pathogenesis-related proteins. *Mol. Plant Pathol.* **2002**, *3*, 135–144. [[CrossRef](#)]
9. Loake, G.; Grant, M. Salicylic acid in plant defence—The players and protagonists. *Curr. Opin. Plant Biol.* **2007**, *10*, 466–472. [[CrossRef](#)]
10. Van Loon, L.C.; Rep, M.; Pieterse, C.M.J. Significance of Inducible Defense-related Proteins in Infected Plants. *Annu. Rev. Phytopathol.* **2006**, *44*, 135–162. [[CrossRef](#)] [[PubMed](#)]
11. Wang, J.-E.; Li, D.-W.; Zhang, Y.-L.; Zhao, Q.; He, Y.-M.; Gong, Z.-H. Defence responses of pepper (*Capsicum annuum* L.) infected with incompatible and compatible strains of *Phytophthora capsici*. *Eur. J. Plant Pathol.* **2013**, *136*, 625–638. [[CrossRef](#)]
12. Akbudak, M.A.; Yildiz, S.; Filiz, E. Pathogenesis related protein-1 (PR-1) genes in tomato (*Solanum lycopersicum* L.): Bioinformatics analyses and expression profiles in response to drought stress. *Genomics* **2020**, *112*, 4089–4099. [[CrossRef](#)]
13. Breen, S.; Williams, S.; Outram, M.; Kobe, B.; Solomon, P.S. Emerging Insights into the Functions of Pathogenesis-Related Protein 1. *Trends Plant Sci.* **2017**, *22*, 871–879. [[CrossRef](#)] [[PubMed](#)]
14. Kiba, A.; Nishihara, M.; Nakatsuka, T.; Yamamura, S. Pathogenesis-related protein 1 homologue is an antifungal protein in Wasabia japonica leaves and confers resistance to *Botrytis cinerea* in transgenic tobacco. *Plant Biotechnol.* **2007**, *24*, 247–253. [[CrossRef](#)]
15. Sarowar, S.; Young, J.K.; Eui, N.K.; Ki, D.K.; Byung, K.H.; Islam, R.; Jeong, S.S. Overexpression of a pepper basic pathogenesis-related protein 1 gene in tobacco plants enhances resistance to heavy metal and pathogen stresses. *Plant Cell Rep.* **2005**, *24*, 216–224. [[CrossRef](#)]
16. Shin, S.H.; Pak, J.-H.; Kim, M.J.; Kim, H.J.; Oh, J.S.; Choi, H.K.; Jung-Hun, P.; Chung, Y.S. An Acidic PATHOGENESIS-RELATED1 Gene of *Oryza grandiglumis* is Involved in Disease Resistance Response Against Bacterial Infection. *Plant Pathol. J.* **2014**, *30*, 208–214. [[CrossRef](#)] [[PubMed](#)]
17. Cooper, B.; Clarke, J.D.; Budworth, P.; Kreps, J.; Hutchison, D.; Park, S.; Guimil, S.; Dunn, M.; Luginbühl, P.; Ellero, C.; et al. A network of rice genes associated with stress response and seed development. *Proc. Natl. Acad. Sci. USA* **2003**, *100*, 4945–4950. [[CrossRef](#)]
18. Lotan, T.; Ori, N.; Fluhr, R. Pathogenesis-related proteins are developmentally regulated in tobacco flowers. *Plant Cell* **1989**, *1*, 881–887.
19. Chen, Y.L.; Lee, C.Y.; Cheng, K.T.; Chang, W.H.; Huang, R.N.; Nam, H.G.; Chen, Y.R. Quantitative peptidomics study reveals that a wound-induced peptide from PR-1 regulates immune signaling in tomato. *Plant Cell* **2014**, *26*, 4135–4148. [[CrossRef](#)]
20. Gamir, J.; Darwiche, R.; Hof, P.V.; Choudhary, V.; Stumpe, M.; Schneider, R.; Mauch, F. The sterol-binding activity of PATHOGENESIS-RELATED PROTEIN 1 reveals the mode of action of an antimicrobial protein. *Plant J.* **2017**, *89*, 502–509. [[CrossRef](#)] [[PubMed](#)]
21. Asha, S.; Sreekumar, S.; Soniya, E.V. Unravelling the complexity of microRNA-mediated gene regulation in black pepper (*Piper nigrum* L.) using high-throughput small RNA profiling. *Plant Cell Rep.* **2016**, *35*, 53–63. [[CrossRef](#)]
22. Hu, L.; Xu, Z.; Wang, M.; Fan, R.; Yuan, D.; Wu, B.; Wu, H.; Qin, X.; Yan, L.; Tan, L.; et al. The chromosome-scale reference genome of black pepper provides insight into piperine biosynthesis. *Nat. Commun.* **2019**, *10*, 1–11. [[CrossRef](#)]
23. Hall, T.A. BIOEDIT: A user-friendly biological sequence alignment editor and analysis program for Windows 95/98/NT. In *Nucleic Acids Symposium Series*; Information Retrieval Ltd.: London, UK, 1999.
24. Marchler-Bauer, A.; Derbyshire, M.K.; Gonzales, N.R.; Lu, S.; Chitsaz, F.; Geer, L.Y.; Geer, R.C.; He, J.; Gwadz, M.; Hurwitz, D.I.; et al. CDD: NCBI's conserved domain database. *Nucleic Acids Res.* **2015**, *43*, D222–D226. [[CrossRef](#)] [[PubMed](#)]
25. Bailey, T.L.; Johnson, J.; Grant, C.E.; Noble, W.S. The MEME Suite. *Nucleic Acids Res.* **2015**, *43*, W39–W49. [[CrossRef](#)]
26. Törönen, P.; Medlar, A.; Holm, L. PANNZER2: A rapid functional annotation web server. *Nucleic Acids Res.* **2018**, *46*, W84–W88. [[CrossRef](#)] [[PubMed](#)]

27. Kanehisa, M.; Sato, Y.; Morishima, K. BlastKOALA and GhostKOALA: KEGG Tools for Functional Characterization of Genome and Metagenome Sequences. *J. Mol. Biol.* **2016**, *428*, 726–731. [[CrossRef](#)]
28. Kelley, L.A.; Mezulis, S.; Yates, C.M.; Wass, M.; Sternberg, M.J.E. The Phyre2 web portal for protein modeling, prediction and analysis. *Nat. Protoc.* **2015**, *10*, 845–858. [[CrossRef](#)]
29. Dundas, J.; Ouyang, Z.; Tseng, J.; Binkowski, A.; Turpaz, Y.; Liang, J. CASTp: Computed atlas of surface topography of proteins with structural and topographical mapping of functionally annotated residues. *Nucleic Acids Res.* **2006**, *34*, W116–W118. [[CrossRef](#)]
30. Fernández-Bautista, N.; Domínguez-Núñez, J.; Moreno, M.M.; Berrocal-Lobo, M. Plant Tissue Trypan Blue Staining during Phytopathogen Infection. *Bio-Protocol* **2016**, *6*. [[CrossRef](#)]
31. Asha, S.; Soniya, E.V. Transfer RNA Derived Small RNAs Targeting Defense Responsive Genes Are Induced during *Phytophthora capsici* Infection in Black Pepper (*Piper nigrum* L.). *Front. Plant Sci.* **2016**, *7*, 1–16. [[CrossRef](#)]
32. Livak, K.J.; Schmittgen, T.D. Analysis of relative gene expression data using real-time quantitative PCR and the 2(-DeltaDeltaC(T)) Method. *Methods* **2001**, *25*, 402–408. [[CrossRef](#)]
33. Higo, K.; Ugawa, Y.; Iwamoto, M.; Korenaga, T. Plant cis-acting regulatory DNA elements (PLACE) database: 1999. *Nucleic Acids Res.* **1999**, *27*, 297–300. [[CrossRef](#)] [[PubMed](#)]
34. Kaur, A.; Pati, P.K.; Pati, A.M.; Nagpal, A.K. In-silico analysis of cis-acting regulatory elements of pathogenesis-related proteins of *Arabidopsis thaliana* and *Oryza sativa*. *PLoS ONE* **2017**, *12*, e0184523. [[CrossRef](#)]
35. Agrios, G.N. How plants defend themselves against pathogens. In *Plant Pathology*, 5th ed.; Elsevier Academic Press: Amsterdam, The Netherlands, 2005.
36. Van Loon, L.C.; Gerritsen, Y.A.M.; Ritter, C.E. Identification, purification, and characterization of pathogenesis-related proteins from virus-infected Samsun NN tobacco leaves. *Plant Mol. Biol.* **1987**, *9*, 593–609. [[CrossRef](#)]
37. Van Loon, L.C.; Pierpoint, W.S.; Boller, T.; Conejero, V. Recommendations for naming plant pathogenesis-related proteins. *Plant Mol. Biol. Rep.* **1994**, *12*, 245–264. [[CrossRef](#)]
38. Memelink, J.; Linthorst, H.J.M.; Schilperoort, R.A.; Hoge, J.H.C. Tobacco genes encoding acidic and basic isoforms of pathogenesis-related proteins display different expression patterns. *Plant Mol. Biol.* **1990**, *14*, 119–126. [[CrossRef](#)] [[PubMed](#)]
39. Mitsuhashi, I.; Iwai, T.; Seo, S.; Yanagawa, Y.; Kawahigasi, H.; Hirose, S.; Ohkawa, Y.; Ohashi, Y. Characteristic expression of twelve rice PR1 family genes in response to pathogen infection, wounding, and defense-related signal compounds (121/180). *Mol. Genet. Genom.* **2008**, *279*, 415–427. [[CrossRef](#)]
40. Almeida-Silva, F.; Venancio, T.M. Pathogenesis-related protein 1 (PR-1) genes in soybean: Genome-wide identification, structural analysis and expression profiling under multiple biotic and abiotic stresses. *bioRxiv* **2021**. [[CrossRef](#)]
41. Choudhary, V.; Darwiche, R.; Gfeller, D.; Zoete, V.; Michielin, O.; Schneiter, R. The caveolin-binding motif of the pathogen-related yeast protein Pry1, a member of the CAP protein superfamily, is required for in vivo export of cholesteryl acetate. *J. Lipid Res.* **2014**, *55*, 883–894. [[CrossRef](#)]
42. Lincoln, J.E.; Sanchez, J.P.; Zumstein, K.; Gilchrist, D.G. Plant and animal PR1 family members inhibit programmed cell death and suppress bacterial pathogens in plant tissues. *Mol. Plant Pathol.* **2018**, *19*, 2111–2123. [[CrossRef](#)]
43. Breen, S.; Williams, S.J.; Winterberg, B.; Kobe, B.; Solomon, P.S. Wheat PR-1 proteins are targeted by necrotrophic pathogen effector proteins. *Plant J.* **2016**, *88*, 13–25. [[CrossRef](#)]
44. Lu, S.; Faris, J.; Sherwood, R.; Friesen, T.L.; Edwards, M.C. A dimeric PR-1-type pathogenesis-related protein interacts with ToxA and potentially mediates ToxA-induced necrosis in sensitive wheat. *Mol. Plant Pathol.* **2014**, *15*, 650–663. [[CrossRef](#)]
45. Danino, Y.M.; Even, D.; Ideses, D.; Juven-Gershon, T. The core promoter: At the heart of gene expression. *Biochim. Biophys. Acta BBA Bioenerg.* **2015**, *1849*, 1116–1131. [[CrossRef](#)]
46. Kaur, G.; Pati, P.K. Analysis of cis-acting regulatory elements of Respiratory burst oxidase homolog ( Rboh ) gene families in *Arabidopsis* and rice provides clues for their diverse functions. *Comput. Biol. Chem.* **2016**, *62*, 104–118. [[CrossRef](#)]
47. Ross, C.; Shen, Q.J. Computational Prediction and Experimental Verification of HVA1-like Abscisic Acid Responsive Promoters in Rice (*Oryza sativa*). *Plant Mol. Biol.* **2006**, *62*, 233–246. [[CrossRef](#)]
48. Kesarwani, M.; Yoo, J.; Dong, X. Genetic Interactions of TGA Transcription Factors in the Regulation of Pathogenesis-Related Genes and Disease Resistance in *Arabidopsis*. *Plant Physiol.* **2007**, *144*, 336–346. [[CrossRef](#)]
49. Fujimoto, S.Y.; Ohta, M.; Usui, A.; Shinshi, H.; Ohme-Takagi, M. *Arabidopsis* ethylene-responsive element binding factors act as transcriptional activators or repressors of GCC box-mediated gene expression. *Plant Cell* **2000**, *12*, 393–404. [[PubMed](#)]
50. Foyer, C.H.; Kerchev, P.I.; Hancock, R.D. The ABA-INSENSITIVE-4 (ABI4) transcription factor links redox, hormone and sugar signaling pathways. *Plant Signal. Behav.* **2012**, *7*, 276–281. [[CrossRef](#)]
51. Akagi, T.; Ikegami, A.; Yonemori, K. DkMyb2 wound-induced transcription factor of persimmon (*Diospyros kaki* Thunb.), contributes to proanthocyanidin regulation. *Planta* **2010**, *232*, 1045–1059. [[CrossRef](#)] [[PubMed](#)]
52. Ryu, K.H.; Kang, Y.H.; Park, Y.H.; Hwang, I.; Schiefelbein, J.; Lee, M.M. The WEREWOLF MYB protein directly regulates CAPRICE transcription during cell fate specification in the *Arabidopsis* root epidermis. *Development* **2005**, *132*, 4765–4775. [[CrossRef](#)] [[PubMed](#)]
53. Taoka, K.-I.; Ohtsubo, N.; Fujimoto, Y.; Mikami, K.; Meshi, T.; Iwabuchi, M. The Modular Structure and Function of the Wheat H1 Promoter with S Phase-Specific Activity. *Plant Cell Physiol.* **1998**, *39*, 294–306. [[CrossRef](#)]

54. Ali, S.; Mir, Z.A.; Bhat, J.A.; Tyagi, A.; Chandrashekar, N.; Yadav, P.; Rawat, S.; Sultana, M.; Grover, A. Isolation and characterization of systemic acquired resistance marker gene PR1 and its promoter from *Brassica juncea*. *3 Biotech* **2018**, *8*, 10. [[CrossRef](#)] [[PubMed](#)]
55. Tunsagool, P.; Jutidamrongphan, W.; Phaonakrop, N.; Jaresitthikunchai, J.; Roytrakul, S.; Leelasuphakul, W. Insights into stress responses in mandarins triggered by *Bacillus subtilis* cyclic lipopeptides and exogenous plant hormones upon *Penicillium digitatum* infection. *Plant Cell Rep.* **2019**, *38*, 559–575. [[CrossRef](#)]
56. Ali, S.; Mir, Z.A.; Tyagi, A.; Bhat, J.A.; Chandrashekar, N.; Papolu, P.K.; Rawat, S.; Grover, A. Identification and comparative analysis of *Brassica juncea* pathogenesis-related genes in response to hormonal, biotic and abiotic stresses. *Acta Physiol. Plant.* **2017**, *39*, 268. [[CrossRef](#)]
57. Seo, P.J.; Kim, M.J.; Park, J.-Y.; Kim, S.-Y.; Jeon, J.; Lee, Y.-H.; Kim, J.; Park, C.-M. Cold activation of a plasma membrane-tethered NAC transcription factor induces a pathogen resistance response in Arabidopsis. *Plant J.* **2010**, *61*, 661–671. [[CrossRef](#)] [[PubMed](#)]
58. Kothari, K.S.; Dansana, P.K.; Giri, J.; Tyagi, A.K. Rice Stress Associated Protein 1 (OsSAP1) Interacts with Aminotransferase (OsAMTR1) and Pathogenesis-Related 1a Protein (OsSCP) and Regulates Abiotic Stress Responses. *Front. Plant Sci.* **2016**, *7*, 1057. [[CrossRef](#)] [[PubMed](#)]
59. Liu, W.-X.; Zhang, F.-C.; Zhang, W.-Z.; Song, L.-F.; Wu, W.-H.; Chen, Y.-F. Arabidopsis Di19 Functions as a Transcription Factor and Modulates PR1, PR2, and PR5 Expression in Response to Drought Stress. *Mol. Plant* **2013**, *6*, 1487–1502. [[CrossRef](#)]
60. Nazeem, P.A.; Achuthan, C.R.; Babu, T.D.; Parab, G.V.; Girija, D.; Keshavachandran, R.; Samiyappan, R. Expression of pathogenesis related proteins in black pepper (*Piper nigrum* L.) in relation to Phytophthora foot rot disease. *J. Trop. Agric.* **2008**, *46*, 45–51.
61. Trang Anh, T.; Bao Linh, T.; Vu Phong, N.; Lan Thanh Bien, T.; Thi Nha Tram, T.; Dinh Don, L. Expression of Proteins Related to *Phytophthora capsici* Tolerance in Black Pepper (*Piper nigrum* L.). *Int. J. Agric. Innov. Res.* **2018**, *6*, 2319–1473.
62. Vijesh Kumar, I.P.; Johnson, G.K.; Anandaraj, M. Real-Time Quantitative RT-PCR of Some Defense Inoculated with *Phytophthora Capsici*. *Int. J. Agric. Sci. Res.* **2016**, *6*, 69–78.